

## Oscillatory Exchange Coupling and Giant Positive Magnetoresistance in TiN/Fe<sub>3</sub>O<sub>4</sub> Superlattices

A. Orozco,\* S. B. Ogale, Y. H. Li, P. Fournier, Eric Li, H. Asano, V. Smolyaninova, R. L. Greene, R. P. Sharma, R. Ramesh, and T. Venkatesan

*NSF-MRSEC on Oxides, Surfaces and Probes and Center for Superconductivity Research, Department of Physics, University of Maryland, College Park, Maryland 20742-4111*

(Received 14 April 1999)

Oscillatory exchange coupling is observed in TiN/Fe<sub>3</sub>O<sub>4</sub> superlattices over length scales comparable to metallic superlattices. However, the strength of the coupling is almost an order of magnitude stronger than that commonly observed in metallic superlattices. In addition, a unique positive magnetoresistance effect is also seen. These observations are discussed in terms of the carrier confinement effects caused by the half metallicity of the magnetic layers.

PACS numbers: 75.70.Cn, 75.30.Et

The exchange coupling between two magnetic layers separated by a thin nonmagnetic layer is seen to oscillate as a function of the thickness of nonmagnetic layer and the oscillation amplitude is seen to damp with increasing thickness [1]. Initial attempts to explain this phenomenon using free electron RKKY-type models predicted periods of oscillation  $\approx \pi/k_F$ , much shorter than the commonly observed periods ( $\approx 10$  Å) [2]. Subsequent work brought out the fact that the discrete nature of the variable spacer thickness leads to long periods due to aliasing. It is now accepted that the oscillation periods are determined by the extremal Fermi surface spanning vectors (connecting critical points on the spacer layer Fermi surface), while the properties of magnetic layers mainly influence the amplitudes and phases of the oscillations [3]. Recently, Bruno [4] and Stiles [5] have shown that the coupling can be described in terms of the quantum interference due to spin dependent reflections of Bloch waves at the interfaces. The interest in this subject continues to grow as evidenced by several recent papers [6–13], which cover interesting issues such as the effect of cap layer, ordering in alloy layers, quantum oscillations of spin density, etc.

Interestingly, the entire research on oscillatory coupling is thus far concentrated only upon pure metals or metal alloys. As is well known, oxides display a very broad range of electrical properties from insulating to superconducting. The magnetic phenomena in oxides also have several facets, with the underlying mechanisms covering direct exchange, superexchange, and double exchange. There is also a wide variety of half metallic oxides such as the manganites, magnetites, molybdates, rhenites, etc., where 100% spin polarization is seen at Fermi level. In spite of such richness of available property space, it is surprising that hardly any studies have yet been reported on oscillatory exchange coupling in heterostructures based on oxides or other compounds. One possible cause for this may be the difficulties encountered in realizing perfect interfaces of defect-free ultrathin films of dissimilar systems of oxides or other compounds. Indeed, all previous attempts at

observing oscillatory coupling in compounds have failed [14,15]. In this work, we demonstrate for the first time that oscillatory exchange coupling effects can be realized in magnetic oxide based heterostructures, provided superlattices (SL) with high quality interfaces can be grown. We also observe an entirely unique giant positive magnetoresistance (MR) effect that we attribute to a high spin polarization of the magnetic layer that cannot be realized in the pure metallic systems. In this work, magnetite (Fe<sub>3</sub>O<sub>4</sub>) was used as the magnetic layer and TiN as the spacer layer.

Fe<sub>3</sub>O<sub>4</sub> is a ferrimagnet with eight tetrahedral *A* sites (all Fe<sup>3+</sup>) and sixteen octahedral *B* sites shared equally by Fe<sup>2+</sup> and Fe<sup>3+</sup> ions. The *d* electron on each octahedral site is the carrier, and it is delocalized in a narrow, spin polarized *t*<sub>2g</sub> minority band above the Verwey transition, rendering half-metallic character to the compound. The exchange between *A* and *B* sites ( $J_{AB} \approx -28$  K) is the strongest and is antiferromagnetic. Thus the Fe<sup>3+</sup> moments on *A* and *B* sites cancel each other, and the net magnetic moment originates due to Fe<sup>2+</sup> ions on *B* sites.

TiN is an interesting metal ( $\rho_{300\text{K}} \approx 30 \mu\Omega \text{ cm}$ ) with a complex bonding composed of localized metal-metal and metal-nonmetal interactions resembling metallic as well as covalent bonding, and a small contribution of ionic bonding. The conduction band has two broad humps corresponding to the bonding and antibonding mixtures of the Ti 3*d*<sup>2</sup> and N 2*p*<sup>3</sup> states. The topology of the Fermi surface is such that the constant energy intersection at the Fermi level with the {100} plane shows cross-shaped contours. It also has a lattice constant very close to half of that for Fe<sub>3</sub>O<sub>4</sub>, ensuring epitaxial compatibility.

We used pulsed laser deposition to grow both Fe<sub>3</sub>O<sub>4</sub> and TiN layers. The films were grown in high vacuum [ $(2-4) \times 10^{-7}$  Torr] at a substrate temperature of 673 K on (100) MgAl<sub>2</sub>O<sub>4</sub>. The growth optimization will be reported separately [16]. Superlattices (50 periods) with magnetic layer of fixed thickness ( $t_{\text{Fe}_3\text{O}_4} = 40$  Å) and changing metallic spacer thicknesses ( $t_{\text{TiN}} = 5, 6, 8, 10, 12, 14, 16, 18, 20, \text{ and } 24$  Å) were deposited. These were

then studied using x-ray diffraction, high resolution and cross-sectional transmission electron microscopy (TEM), atomic force microscopy (AFM), Rutherford backscattering (RBS), vibrating sample magnetometry, SQUID magnetometry, and four probe resistivity with and without an applied magnetic field.

Under the selected deposition conditions the AFM pictures (not shown) revealed extremely flat surfaces with average roughness less than  $3 \text{ \AA}$  over a  $3 \times 3 \mu\text{m}^2$  square area. The film thicknesses were confirmed using RBS spectroscopy. Figure 1 shows a cross-section TEM micrograph of a typical TiN/Fe<sub>3</sub>O<sub>4</sub> film, revealing flat interfaces [17]. The diffraction pattern shown in the lower inset verifies the cubic structure of Fe<sub>3</sub>O<sub>4</sub> and TiN, revealing good epitaxy. The high resolution picture in the upper inset exhibits the high interfacial quality.

Representative data on the room temperature magnetization versus in-plane applied magnetic field up to 1 T are shown in Fig. 2 for a few values of TiN thicknesses (5, 8, and 14 Å). The oscillation in the shape of the hysteresis loop is clear. The absence of multiple values of coercivities in all SL is indicative of the existence of interlayer coupling between magnetic layers [18,19]. The saturation magnetization of the Fe<sub>3</sub>O<sub>4</sub> subsystem was found to be very close to that of pure Fe<sub>3</sub>O<sub>4</sub> single layer of total thickness equivalent to the amount of Fe<sub>3</sub>O<sub>4</sub> in the film, in all SL. Thus, the change in the saturation field  $H_s$  can be understood as reflecting the more fundamental oscillation in the exchange interlayer coupling. Figure 3 clearly shows the remarkable oscillatory behavior of  $H_s$ , exhibiting a pronounced peak around 8 Å, followed by a weaker one around 19 Å, giving an estimated oscillation period of about  $11 \pm 1 \text{ \AA}$ , similar to the long-period oscillation found in most of the different metallic SL [2]. It is remarkable that in spite of a cross-shaped topology of the TiN Fermi surface, the observed long period in our (100) oriented configuration is comparable to

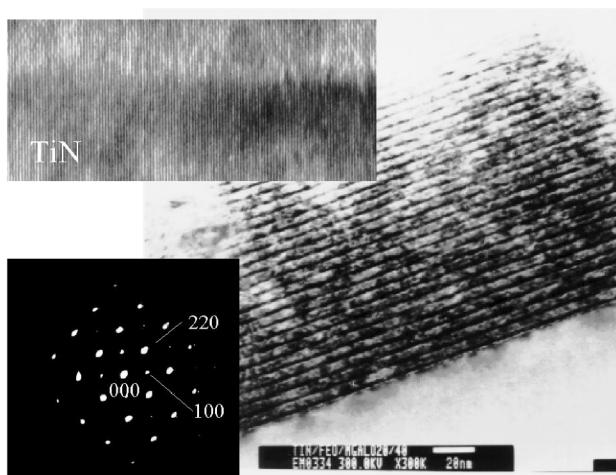


FIG. 1. TEM cross-section and diffraction pattern of TiN/Fe<sub>3</sub>O<sub>4</sub> superlattice. See text.

that seen in metallic SL involving noble metal spacers with nearly spherical Fermi surfaces. The saturation field  $H_s$  reflects the strength of the interlayer exchange coupling  $J_i = H_s M_s t_{\text{Fe}_3\text{O}_4} / 2$  [20]. The estimated value of coupling strength  $J_i \approx 1.33 \text{ mJ/m}^2$  is clearly remarkably higher than the largest strength found in most metallic structures [1]. As we discuss below, the high strength of the coupling should originate from the half metallicity of the magnetic layer.

The dynamics of carriers in the modulated structures, which are crucial for the exchange coupling and magnetotransport, are essentially governed by the nature of matching of band structures along the specific crystallographic orientation of modulation. Comparison of Fe<sub>3</sub>O<sub>4</sub> and TiN band structures [21,22] shows that the majority and minority carriers experience a mismatch along (100) which is seen as potential barriers with different heights for the two spin subbands. These barriers can confine the electrons in several layers, because the partial reflection coefficient for the states inside the well can yield quantum well resonances giving rise to discrete states. Such resonances have indeed been observed by photoemission experiments [23,24]. Furthermore, the accessible states near the Fermi level are an additional restriction because of the half-metallicity of Fe<sub>3</sub>O<sub>4</sub>, making the confinement stronger for the majority case. The difference in reflection

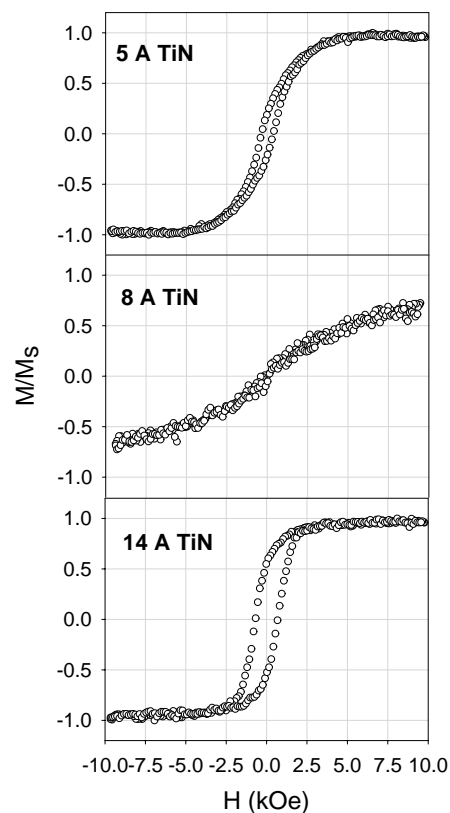


FIG. 2. Room temperature magnetization vs magnetic field for TiN/Fe<sub>3</sub>O<sub>4</sub> SL with 5, 8, and 14 Å TiN thicknesses.

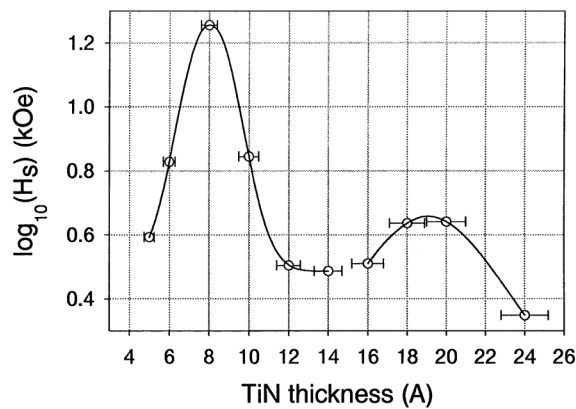


FIG. 3. Oscillatory exchange coupling as a function of the TiN spacer thickness.

coefficients for the two spins can be considered the cause for the spin-dependent scattering at the interfaces. Moreover, the quantum confinement of the spin polarized electrons leads to fluctuations of the interlayer exchange coupling, as discussed by Barnas [25] and Bruno [4], and the strength of the coupling depends directly on the spin asymmetry reflection probabilities at the interfaces [4]. This way, the higher spin polarization of  $\text{Fe}_3\text{O}_4$  can result in a higher value of the former quantity and, thus, in the strength of coupling as we observe in this system.

We performed high-field current-in-plane (CIP) magnetoresistance measurements (up to  $\approx 8.5$  T) at 300 and 150 K, with the magnetic field applied in the plane of the films. In the present study, we restricted the low temperature measurement to 150 K so as to avoid crossing of the Verwey transition temperature of  $\text{Fe}_3\text{O}_4 \approx 120$  K. At this temperature, the B sites in  $\text{Fe}_3\text{O}_4$  undergo a first order transition to a charge ordered state. This state has distinctly different carrier dynamics and enhanced spin density ordering which should influence the magnetoresistance as well as the exchange coupling. These aspects will be explored in future work. Figure 4 shows the results for the sample  $[\text{TiN}(10 \text{ \AA})/\text{Fe}_3\text{O}_4(40 \text{ \AA})]_{50}$ . A remarkable large positive magnetoresistance is seen; the values being  $\approx 5.6\%$  at 150 K and  $\approx 6.5\%$  at 300 K in a field of  $\approx 8$  T. In both cases we can distinguish two regions: one within the interval  $\approx \pm 1$  T, separated by a sudden jump (of about 1% at 150 K), from another exhibiting almost linear increase in resistance with the magnetic field. We must notice that the sharp jump in resistance occurs in both cases at field values  $\pm 1$  T, very close to the  $H_s$  for the sample. The presence of hysteresis can also be noted in MR, as has been observed in metallic SL systems. We point out here that the observed positive MR in the case of our TiN/ $\text{Fe}_3\text{O}_4$  superlattice is distinctly different as compared to the negative MR observed in the case of single layer  $\text{Fe}_3\text{O}_4$  film, as reported by us previously [26]. In the latter case of single layer  $\text{Fe}_3\text{O}_4$  film, the transport at temperatures above the Verwey transition

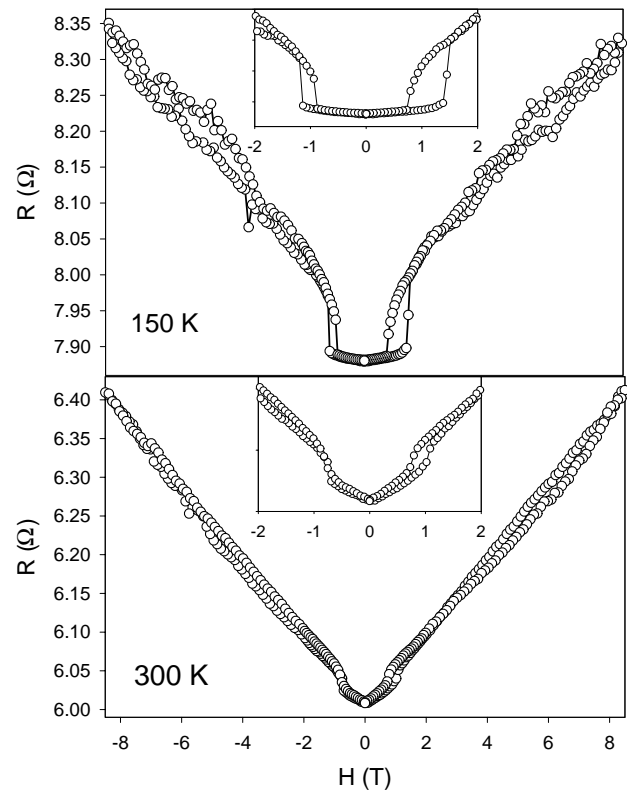


FIG. 4. CIP magnetoresistance at 150 K and room temperature for the  $[\text{TiN}(10 \text{ \AA})/\text{Fe}_3\text{O}_4(40 \text{ \AA})]_{50}$  superlattice.

up to the room temperature (the range examined here) has been attributed to a small polaron hopping mechanism, and application of magnetic field is suggested to broaden the small polaronic band leading to enhanced conduction, and thereby a negative MR [27]. The opposite sign of MR as well as the occurrence of the jump in the resistance at the saturation field uniquely reflect the interlayer origin of the observed positive MR effect in the superlattice.

Within this quantum confinement picture, we can try to understand the origin of the positive MR. The simplest way is to make use of a phenomenological network resistor model. We consider two situations; one (referred to as AFMC) for  $H < H_s$  for which the magnetic layers are coupled antiferromagnetically, and another (referred to as FMC) for  $H > H_s$ , when the layers are coupled ferromagnetically. In the SL, the magnetic layers, namely,  $\text{Fe}_3\text{O}_4$ , have a minority spin band near the Fermi energy. Let us assume that the spacer metallic layer has no spin polarization, which is applicable to the TiN case.

In the AFMC case, a carrier with a given spin orientation (opposite to the magnetization of  $\text{Fe}_3\text{O}_4$  layer due to minority character) finds accessible states in the three layer system comprising one  $\text{Fe}_3\text{O}_4$  layer sandwiched between two TiN layers. The carrier with an opposite spin orientation also finds a similar three layer transport space. In this way all the carriers in the system are sampled in three layer stacks, with interface scattering

effects experienced mainly at every fourth interface. In order to infer the compounded effect on transport one can use a value of mean conductivity weighted by the layer thicknesses.

In the FMC case, since the magnetization of all  $\text{Fe}_3\text{O}_4$  layers are parallel, the minority carriers can find accessible states throughout the stack, while the carriers with an opposing spin orientation present only in TiN have to restrict themselves to the TiN spacer layers to which they belong. The minority carriers will therefore experience a mean conductivity of the whole stack within the mean free path, while the majority carriers will experience a high degree of interface scattering, reflecting the conductivity corresponding to an ultrathin spacer layer. Quantum size effects as well as magnetic layer proximity effects in defining the electron states in the spacer layer would have to be incorporated in a more rigorous analysis. The 50% of TiN carriers (minority) will thus experience the mean conductivity of the full stack. This channel will operate in parallel with the channel provided by the remaining 50% majority carriers, using a resistivity value for ultrathin film ( $\rho''$ ) in this case.

We consider the case of a 50 period  $[\text{TiN}(10 \text{ \AA})/\text{Fe}_3\text{O}_4(40 \text{ \AA})]_{50}$  SL. We take the following experimentally realized values of resistivity at room temperature to make some estimates:  $\rho(\text{Fe}_3\text{O}_4) \approx 7 \text{ m}\Omega \text{ cm}$ ,  $\rho(\text{TiN}) \approx 24 \mu\Omega \text{ cm}$ , and  $\rho''(\text{TiN}) \approx 96.5 \mu\Omega \text{ cm}$ . These numbers give the resistance values for the AFMC and FMC configurations of  $\approx 3.65$  and  $9.2 \Omega$ , respectively. It may be noted that the binding interfaces for the TiN/ $\text{Fe}_3\text{O}_4$ /TiN trilayer configurations in the AFMC case would lead to additional magnetic scattering and increase the resistance to a value higher than  $3.65 \Omega$ , say,  $(1 + \alpha)3.65 \Omega$ . We do not expect  $\alpha$  to be more than unity. Thus, application of magnetic field which would change the configuration from AFMC to FMC can lead to a positive magnetoresistance in this case, as observed in our experiment. The estimated resistance values are also in a good agreement with the experimentally obtained values. It is useful to point out that large positive MR effects have been reported recently in trilayer oxide structures [28,29].

In summary, we report oscillatory behavior of the interlayer coupling in an all-compound superlattice system. The strength of the coupling is remarkably higher than that observed commonly in metallic superlattices. In addition, a unique large positive CIP-MR is seen. It is argued that the high spin polarization of the magnetic system and related spin selective quantum confinement effects in the heterostructure are responsible for the high strength of exchange coupling and the positive magnetoresistance.

We thank J. Cullen for critical reading of the manuscript, and C.M. Innes and C. Galley for their help. This work was supported by NSF-MRSEC under Grant No. DMR-96-32521, DARPA Contract No. N000149610770, and the FPI program of the MEC (Spain).

\*Email address: antonio@squid.umd.edu

- [1] *Ultrathin Magnetic Structures*, edited by J.A.C. Bland and B. Heinrich (Springer-Verlag, Berlin, 1994).
- [2] S.S.P. Parkin, Phys. Rev. Lett. **67**, 3598 (1991).
- [3] P. Bruno and C. Chappert, Phys. Rev. B **46**, 261 (1992).
- [4] P. Bruno, Phys. Rev. B **52**, 411 (1995).
- [5] M.D. Stiles, Phys. Rev. B **48**, 7238 (1993).
- [6] J.J. de Vries *et al.*, Phys. Rev. Lett. **75**, 4306 (1995).
- [7] M. van Schilfgaarde, F. Herman, S.S.P. Parkin, and J. Kudrnovsky, Phys. Rev. Lett. **74**, 4063 (1995).
- [8] J. Kudrnovsky *et al.*, Phys. Rev. Lett. **76**, 3834 (1996).
- [9] M.A. Tomaz, J.W.J. Antel, W.L. O'Brien, and G.R. Harp, Phys. Rev. B **55**, 3716 (1997).
- [10] A.J.R. Ives, J.A.C. Bland, R.J. Hicken, and C. Daboo, Phys. Rev. B **55**, 12 428 (1997).
- [11] P. Fuchs, U. Ramsperger, A. Vaterlaus, and M. Landolt, Phys. Rev. B **55**, 12 546 (1997).
- [12] U. Ebels *et al.*, Phys. Rev. B **58**, 6367 (1998).
- [13] J. Mathon, A. Umerski, and M. Villeret, Phys. Rev. B **59**, 6344 (1999).
- [14] J.E. Mattson *et al.*, Phys. Rev. B **55**, 70 (1997).
- [15] C.A.R.S. de Melo, Phys. Rev. Lett. **79**, 1933 (1997).
- [16] A. Orozco *et al.* (unpublished).
- [17] The variation in contrast in the TEM picture is due to *e*-beam induced damage in  $\text{Fe}_3\text{O}_4$ .
- [18] S.R. Herd and K.Y. Ahn, J. Appl. Phys. **50**, 2384 (1979).
- [19] N. Kumasaka *et al.*, J. Appl. Phys. **55**, 2238 (1984).
- [20] F.N. van Dau *et al.*, J. Phys. (Paris), Colloq. **48**, C8 (1988).
- [21] M. Penicaud, B. Siberchicot, C.B. Sommers, and J. Kubler, J. Magn. Magn. Mater. **103**, 212 (1992).
- [22] R. Ahuja, O. Eriksson, J.M. Wills, and B. Johansson, Phys. Rev. B **53**, 3072 (1996).
- [23] J.E. Ortega and F.J. Himpsel, Phys. Rev. Lett. **69**, 844 (1992).
- [24] J.E. Ortega, F.J. Himpsel, G.J. Mankey, and R.F. Willis, Phys. Rev. B **47**, 1540 (1993).
- [25] J. Barnas, J. Magn. Magn. Mater. **111**, L215 (1992).
- [26] S.B. Ogale *et al.*, Phys. Rev. B **57**, 7823 (1998).
- [27] D. Ihle and B. Lorenz, J. Phys. C **19**, 5239 (1986).
- [28] M.R.J. Gibbs *et al.*, Philos. Trans. R. Soc. London A **356**, 1681 (1998).
- [29] K. Ghosh *et al.*, Appl. Phys. Lett. **73**, 689 (1998).